JOURNAL OF SOLID STATE CHEMISTRY 72, 244–256 (1988)

Energetics of Compounds ($A^{2+}B^{4+}O_3$) with the Perovskite Structure

EIJI TAKAYAMA-MUROMACHI

National Institute for Research in Inorganic Materials (NIRIM), Sakura, Niihari, Ibaraki 305, Japan

AND ALEXANDRA NAVROTSKY

Department of Geological and Geophysical Sciences, Princeton University, Princeton, New Jersey 08544

Received October 6, 1986; in revised form May 18, 1987

The heats of formation from oxides for perovskite compounds, ABO_3 (A = Ca, Sr, Ba, Pb, Cd, B = Ti, Zr), were determined by high-temperature solution calorimetry using an alkali borate solvent. The values obtained agree with the results of earlier HF solution calorimetry, when available. The heat of formation from the oxides generally becomes more negative the closer the tolerance factor for that perovskite is to unity. The heat of formation can be divided into two contributions, that from changes in electrostatic (Madelung) energy, which becomes more negative as the tolerance factor decreases from 1 to ~0.8, reflecting a smaller volume for the perovskite, and that from other energy terms, mainly repulsive interactions. The change in these terms is generally positive, reflecting greater repulsion in the perovskite structure than in the binary oxides, and increases with increasing deviation of the tolerance factor from unity. These energy terms also correlate with the apparent contraction of the octahedral sublattice relative to that calculated for ideal geometry. From the heats of solution of the polymorphs of $CdTiO_3$ and $BaTiO_3$, the heat of transition between ilmenite- and perovskite-type $CdTiO_3$ and that between perovskite- and high-temperature hexagonal-type $BaTiO_3$ were calculated to be 8.2 ± 2.3 and 5.6 ± 3.4 kJ/mole.

Introduction

Many compounds with the general formula ABO_3 have the perovskite structure. The ideal perovskite structure has a cubic unit cell with space group $Pm3m$, and the A cation is coordinated by 12 oxygen ions and the B cation by 6. Although few perovskite-type oxides have the simple cubic structure at room temperature, many take this ideal structure at elevated temperatures.

Compounds having the perovskite or perovskite-related structure exhibit several technologically interesting physical properties such as ferroelectricity, ferromagnetism, and weak ferromagnetism (*1*), as well as superconductivity (*53*). In addition, silicate perovskite of composition $Fe_xMg_{1-x}SiO_3$ ($0 < x < \sim 0.2$) may be the dominant phase in the earth's lower mantle (*2*), giving the perovskite structure considerable geophysical interest. Recent high-pressure experiments reveal that several metasilicates, $ASiO_3$, and metagermanates, $AGeO_3$, transform to the perovskite structure at high pressure (*3*).

The heats of formation of some perovskite compounds from binary oxides

0022-4596/88 $3.00

have been determined by HF solution calorimetry (see Table IV). While HF solution calorimetry is still the usual method for hydrous compounds, oxide melt solution calorimetry has become the more powerful method for many anhydrous oxides (*4*). In this work, oxide melt solution calorimetry using an alkali borate solvent was applied to obtain the heat of formation from the oxides for $A^{2+}B^{4+}O_3$-type perovskites (A = Ca, Sr, Ba, Pb, Cd, B = Ti, Zr). The present results were compared with earlier values from HF solution calorimetry with which they generally agree. The data, now available for a larger number of perovskites, have been interpreted in terms of crystal–chemical systematics, especially the role of the tolerance factor and of Madelung and repulsive (or nonelectrostatic) energies. In addition, the cubic–hexagonal transition in $BaTiO_3$ and the ilmenite–perovskite transition in $CdTiO_3$ have been studied.

Experimental Methods

Sample Preparation

Dried reagent-grade TiO_2 (rutile type), ZrO_2 (baddeleyite type), $CaCO_3$, $SrCO_3$, $BaCO_3$, PbO (yellow form), and CdO were used as starting materials. The perovskite compounds which contain alkali earth elements were made by heating equimolar mixture of TiO_2 (ZrO_2) and an alkali earth carbonate at 1423 K for several days with intermediate grindings. To minimize vaporization of lead oxide and cadmium oxide, $PbTiO_3$, $PbZrO_3$, and $CdTiO_3$ were synthesized at 1023 K. Even at this temperature, the reaction rate is large enough to obtain single phases within several days. Since $CdTiO_3$ crystallizes as the ilmenite form at 1023 K (*5*), the perovskite form was made by transforming the ilmenite compound at 1323 K. The transformation occurs completely within a few hours without detectable weight change. Although we tried to make $CdZrO_3$, no compounds were found between CdO and ZrO_2. This absence of compounds may be understood in terms of the observed energy systematics (see below).

In addition to the perovskite-type $BaTiO_3$ sample we synthesized, three other samples were obtained. The first one was a perovskite made by a coprecipitation method (*6*). The precipitate of barium and titanium oxalate was given to us by H. Yamamura of NIRIM and was calcined at 1273 K to get fine powder of perovskite-type $BaTiO_3$. The other two samples were provided by B. Wechsler of Hughes Research Labs. They are high-temperature hexagonal $BaTiO_3$ (*7*) made above 1733 K and a dense perovskite sample sintered at 1673 K. From these samples, we could investigate the influence of preparation temperature on enthalpy of perovskite-type $BaTiO_3$. Moreover, we determined the heat of transition between Ba TiO_3 (perovskite) and $BaTiO_3$ (hexagonal).

To obtain heats of solution of reference materials, CaO and SrO were made by decomposing the corresponding carbonates at 1573 K in a platinum crucible. The monoxides thus obtained were handled carefully to minimize adsorption of H_2O and CO_2 in air. Barium oxide could not be prepared by decomposing $BaCO_3$, because the resulting barium oxide seriously attacks platinum or alumina crucibles. Instead of direct calorimetric measurement of BaO, barium peroxide, which is stable in air at room temperature, was examined, and the heat of solution of BaO was calculated from the data on barium peroxide. Barium peroxide, BaO_2 was prepared from an aqueous solution of BaOH and H_2O_2 (*8*) in an inert gas atmosphere.

All samples were observed to be single-phase perovskites by microscopic examination and by X-ray diffraction. Chemical analysis for minor elements is shown in Table I. All other impurities are present in

TABLE I

CHEMICAL ANALYSIS OF IMPURITY ELEMENTS (wt%)

	Si[a]	Al[b]	Ca[b]	Ti[b]	Co[b]	Sr[c]	Fe[c]
$PbZrO_3$	0.02	0.05	0.02	0.04	0.002		
$SrTiO_3$	0.08	0.01	0.02		0.01		
$BaSnO_3$	0.04	0.003	0.01	0.0008	0.003		
$BaTiO_3$	0.05	0.01	0.02		0.04		
BaO_2	0.002	0.0008	0.004	0.0004	0.0003		
$CaSnO_3$	0.01	0.007		0.001	0.002		
$CaTiO_3$	0.04	0.02			0.01		
$CaZrO_3$	0.04	0.08		0.07	0.001		
$CdTiO_3$(il)	0.02	0.02	0.03		0.01		
$CdTiO_3$(pv)	0.03	0.02	0.06		0.02		
$BaCO_3$						0.0009	
TiO_2	0.0007[c]						0.001

[a] Done at NIRIM by spectrophotometry.

[b] Done at NIRIM by emission ICP spectroscopy.

[c] Johnson–Matthey certificate of analysis for $BaCO_3$ and TiO_2 used in synthesis of B. Wechsler's $BaTiO_3$ samples.

even lower concentrations. In addition, major element analyses were done for $CaSnO_3$, $CaTiO_3$, and $CaZrO_3$. Ca, Sn, and Zr were determined by direct or back titration with EDTA, Ti by thermogravimetry using cupferron. The results are shown in Table II.

Calorimetric Solvent

The solvent generally used for oxides and silicates, molten $2PbO \cdot B_2O_3$ near 973 K, is unsuitable for compounds containing ZrO_2 and TiO_2 because they rapidly precipitate $PbZrO_3$ or $PbTiO_3$ (themselves perovskites) on contact with high concentrations of PbO in the melt (*4*).

TABLE II

CHEMICAL ANALYSIS OF SELECTED PEROVSKITES (wt%)

	Element			
Compound	Ca	Sn	Ti	Zr
$CaSnO_3$	19.3[a]	57.5		
	(19.38)[b]	(57.41)		
$CaTiO_3$	29.0		35.2	
	(29.48)		(35.22)	
$CaZrO_3$	22.4			50.2
	(22.35)			(50.88)

[a] Analytical result, second number.

[b] Theoretical stoichiometric amount.

Molten sodium molybdate, $3Na_2O \cdot 4MoO_3$, has been previously employed as a solvent for the high-temperature solution calorimetry of TiO_2-bearing samples (*4*); however, it has been pointed out that complete dissolution of samples in the solvent is not easy with the normal method of stirring (*9*). In the present study, we used, therefore, a nearly eutectic mixture of 52 wt% $LiBO_2$ and 48 wt% $NaBO_2$ as solvent. This solvent has already been applied to determine heat of formation of $Fe_3Al_2Si_3O_{12}$ by Chatillon-Colinet *et al.* (*10*).

Reagent-grade hydrated sodium metaborate, $NaBO_2 \cdot xH_2O$, was dehydrated at 453 K in a Teflon dish and dried at 773 K in an alumina dish for 12 h to make $NaBO_2$. Lithium metaborate, $LiBO_2$ was prepared from Li_2CO_3 (99%) and Baker analyzed reagent H_3BO_3 by solid-state reaction at 873 K in an alumina dish.

Mechanically mixed $LiBO_2$ and $NaBO_2$ were melted in a platinum crucible over a

gas torch; then the melt was quenched into a graphite dish. The entire amount of glass thus obtained was pulverized in an agate mortar. This procedure was repeated twice to get homogeneous glass.

Calorimetric Measurements

Solution calorimetry was carried out in a twin Calvet-type microcalorimeter (*4*) maintained at 1068 ± 2 K. A standard amount of 10 g of alkali borate solvent was used in all solution experiments. The weight of the sample was 20–50 mg and as many as five consecutive solution runs were done with the same 10-g batch of solvent. No differences were detected in the heat effect of the first and subsequent solution runs, confirming the observation of Chatillon-Colinet *et al.* (*10*). The calibration of the calorimeter was performed by dropping small platinum pieces into the calorimeter from room temperature (*4*).

In preliminary solution experiments, samples were placed in a small platinum sample holder with a perforated platinum foil bottom (*11*); however, the solvent did not run out through the holes in the foil bottom, causing incomplete dissolution of samples. This may be due to a larger viscosity of the alkali borate than of the lead borate solvent. The holes in the bottom were enlarged enough to let the solvent run out smoothly. To prevent the sample from falling into the flux prematurely through these larger holes, another platinum foil (with no pinholes) was attached below the perforated bottom with two sides open for the solvent to flow out. With this double-bottomed container, relatively little stirring was required to ensure complete dissolution of sample. Complete dissolution of sample was confirmed by visual inspection of the sample container and the solvent after each solution run. The normal shape of the calorimetric curves and consistency of the data also support complete dissolution. Stirring corrections from 1 to 10% of the total heat of reaction were applied to the data.

After being loaded, samples were generally held in the calorimeter for 16 to 20 h before the reactions were begun. The perovskite form of $CdTiO_3$ held at 1068 K for 20 h contained trace amounts of the ilmenite, indicating some back-reaction. We minimized the equilibration time to less than 7 h for perovskite-type $CdTiO_3$. Back-reaction was not observed for high-temperature hexagonal $BaTiO_3$, so it was treated normally.

From the solution experiments for both perovskite- and ilmenite-type $CdTiO_3$, the heat of transition between the two polymorphs was calculated. As described later, the present result is different from the previous one. To reconcile the difference, transposed-temperature-drop calorimetry (*12*) was performed for the polymorphs of $CdTiO_3$ in addition to solution experiments. Preliminary experiments indicated ilmenite-type $CdTiO_3$ transforms to the perovskite form within several minutes by heating at 1333 or 1353 K, and weight loss (CdO vaporization) is negligible within this short period. Thus, the heat of transition can be determined directly by dropping the sample from room temperature into a calorimeter maintained at 1333 or 1353 K and then repeating the experiment on the transformed sample. The difference between these two measurements gives the heat of transition at room temperature. The calorimeter used for this purpose was a commercially available Setaram "HT-1500" type. About 40 mg of sample was wrapped with thin platinum foil (0.0005 in. thick) and dropped into the calorimeter. The detailed procedure has already been described elsewhere (*13*).

Transposed-temperature-drop calorimetry and drop-solution calorimetry were carried out for BaO_2 to obtain the heat of solution of BaO. The barium peroxide sintered tightly at 723 K was broken into small

pieces. A bare BaO_2 piece (without platinum foil wrapping) was dropped from room temperature into the alkali borate solvent in the calorimeter at 1068 K. The heat effect of this drop-solution run corresponds to the following reaction.

$$BaO_2\ (298\ K) \rightarrow BaO\ (solution,\ 1068\ K) + \tfrac{1}{2}O_2\ (gas,\ 1068\ K) \quad (1)$$

Though it was observed visually that BaO_2 dissolves to the alkali borate melt very quickly with evolution of oxygen gas, one could still question whether all the oxygen was released. To check this point, the weight of the BaO_2 piece was varied from 25 to 60 mg, and no correlation was observed between sample weight and molar heat effect. We concluded all oxygen was released from the solvent according to reaction (1). In the drop calorimetry of BaO_2, $BaCO_3$ or MgO was placed (instead of the solvent) in the platinum crucibles located in the calorimeter. This material, unreactive to BaO, was expected to protect the platinum crucible from attack by BaO. Similarly, in the drop solution run, a bare piece of BaO_2 (about 40 mg) was dropped from room temperature into a platinum crucible containing solvent within the calorimeter. It was confirmed that the heat effect, which is expected to correspond to the following reaction, is not affected by the kind of protective material.

$$BaO_2\ (298\ K) \rightarrow BaO\ (1068\ K) + \tfrac{1}{2}O_2\ (gas,\ 1068\ K) \quad (2)$$

Since the solubility of BaO_2 in BaO is low at 1068 K in air (*14*), this reaction is considered to proceed completely. The heat of solution of BaO may then be calculated from the difference between the enthalpy of reactions (1) and (2).

For very basic oxides such as CaO and SrO, one must consider possible absorption of H_2O and CO_2 during sample handling. Though samples were kept in desiccators and the time they were exposed to air was minimized, dry-box techniques were not used. To check whether adsorbed CO_2 or H_2O had any effect on the heat of solution of CaO, solution calorimetry was performed in two different ways. In the first method the normal treatment was applied to CaO previously prepared at 1573 K, while in the second method, $CaCO_3$ was loaded into the calorimeter and decomposed to CaO during the equilibration time prior to calorimetry. As shown in Table III, the two data sets are in good agreement with each other. Though the second method could not be applied to SrO (since $SrCO_3$ does not decompose at 1068 K), it was expected that SrO would act similarly to CaO.

Results and Discussion

Table III shows the heats of solution determined in the present work. The heat of solution of BaO was obtained from the data on BaO_2, which are also shown in the table.

The heats of solution for three kinds of sample of $BaTiO_3$ (perovskite) are identical to each other within experimental error. The preparation temperature does not detectably affect the enthalpy of this compound.

As described previously, perovskite compounds do not always have ideal cubic symmetry, but take distorted structures having orthorhombic, tetragonal, or rhombohedral symmetry depending on temperature. Thus, $BaTiO_3$, while tetragonal at room temperature, is cubic at 1068 K. Therefore, the measured heat of solution for $BaTiO_3$ (perovskite) is that of the cubic form, rather than of the tetragonal form; however, the enthalpy difference between two forms having different symmetry is expected to be small compared with the heat of formation. Thus, we shall neglect the small differences in enthalpy resulting from

TABLE III

HEAT OF SOLUTION IN $LiBO_2$–$NaBO_2$ (52 wt% $LiBO_2$) SOLVENT AT 1068 ± 2 K

Compound	ΔH°_{sol} (kJ/mole)
CaO[c]	−23.46 ± 0.42(3)[a,b]
CaO[d]	−23.54 ± 0.68(5)
CaO (all) (rock salt)	−23.51 ± 0.56(8)
SrO (rock salt)	−59.15 ± 1.08(6)
BaO[e] (rock salt)	−87.94 ± 2.67
BaO_2	[53.48 ± 1.80(6)][f]
BaO_2	[141.42 ± 1.97(5)][g]
PbO (yellow)	42.63 ± 2.29(8)
CdO (rock salt)	36.99 ± 1.63(6)
CdO (rock salt)	[8.70 ± 1.57][h]
TiO_2 (rutile)	39.19 ± 1.38(11)
ZrO_2 (baddeleyite)	44.94 ± 2.62(12)
$CaTiO_3$ (perovskite)	96.53 ± 1.72(5)
$SrTiO_3$ (perovskite)	115.18 ± 1.30(6)
$BaTiO_3$ (perovskite)[i]	103.58 ± 2.74(6)
$BaTiO_3$ (perovskite)[j]	103.26 ± 3.32(4)
$BaTiO_3$ (perovskite)[k]	103.61 ± 2.65(4)
$BaTiO_3$ (perovskite all)	103.50 ± 2.66(14)
$BaTiO_3$ (hexagonal)	97.92 ± 2.12(7)
$PbTiO_3$ (perovskite)	112.89 ± 3.08(5)
$CdTiO_3$ (perovskite)	98.47 ± 1.16(10)
$CdTiO_3$ (ilmenite)	106.70 ± 1.96(5)
$CaZrO_3$ (perovskite)	52.76 ± 2.91(7)
$SrZrO_3$ (perovskite)	61.69 ± 3.49(6)
$BaZrO_3$ (perovskite)	80.85 ± 1.72(6)
$PbZrO_3$ (perovskite)	85.84 ± 5.60(9)

[a] Errors are standard deviations; two significant figures are kept to minimize roundoff errors in further calculations.

[b] Number in parentheses is number of experiments performed.

[c] From decomposition of $CaCO_3$ at 1573 K.

[d] From decomposition of $CaCO_3$ in the calorimeter.

[e] Calculated from the data on BaO_2.

[f] Value from drop solution calorimetry (see text), not a heat of solution.

[g] Value from drop calorimetry (see text), not a heat of solution.

[h] Heat of solution in $2PbO \cdot B_2O_3$ at 987 K.

[i] Prepared at 1423 K.

[j] Prepared by coprecipitation method.

[k] Prepared at 1673 K.

symmetry changes within the perovskite structure in the following discussion.

Heats of Formation

The enthalpy of formation from the oxides was calculated from the heats of solution shown in Table IV. The formation reaction is

$$AO + BO_2 \rightarrow ABO_3. \quad (3)$$

The present values of heats of formation for perovskite compounds are in good agreement with the previous values based on HF solution calorimetry and heat capacities of compounds (*45*). The literature values for the $CdTiO_3$ polymorphs are based on a high-temperature solution experiment using $3Na_2O \cdot 4MoO_3$ solvent (*15*); however, we recalculated the heats of formation using the new value of the heat of solution of TiO_2 (rutile) in $3Na_2O \cdot 4MoO_3$ solvent (*9*), rather than the early value, according to the discussion of Wechsler and Navrotsky (*9*) and Mitsuhashi and Kleppa (*49*). The differences between the present and previous values for $CdTiO_3$ polymorphs is discussed in detail below.

TABLE IV

HEAT OF FORMATION FROM OXIDES (kJ/mole)

Compound	ΔH°_f(1068 K), this work	ΔH°_f, reference
$CaTiO_3$ (perovskite)[a]	−80.9 ± 2.3	−76.0[b]
$SrTiO_3$ (perovskite)	−135.1 ± 2.2	−134.2[b]
$BaTiO_3$ (perovskite)	−152.3 ± 4.0	−153.3[b]
$BaTiO_3$ (hexagonal)	−146.7 ± 3.7	
$PbTiO_3$ (perovskite)	−31.1 ± 4.1	−29.4[b]
$CdTiO_3$ (perovskite)	−22.3 ± 2.4	−7.0 ± 0.9[c]
$CdTiO_3$ (ilmenite)	−30.5 ± 2.9	−22.0 ± 0.7[c]
$CaZrO_3$ (perovskite)	−31.3 ± 4.0	−33.5[b]
$SrZrO_3$ (perovskite)	−75.9 ± 4.5	−77.4[b]
$BaZrO_3$ (perovskite)	−123.9 ± 4.1	−121.3[b]
$PbZrO_3$ (perovskite)	+1.7 ± 6.6	
$CaGeO_3$ (perovskite)		−33.4 ± 3.3[d]
$CdGeO_3$ (perovskite)		+22.6 ± 4.3[d]
$MgSiO_3$ (perovskite)		[+31 ± 20][e]

[a] TiO_2, GeO_2, SiO_2 in rutile structure, ZrO_2 baddeleyite, AO rock salt except for PbO ("yellow").

[b] ΔH°_f (1068 K) from Ref. (*45*).

[c] ΔH°_f (965 K) from Ref. (*15*).

[d] From high-temperature calorimetry of polymorphs (*16, 17*).

[e] Estimated from enthalpy of formation of $MgSiO_3$ (pyroxene) from MgO + SiO_2 (quartz) (*46*), enthalpy of SiO_2 (quartz → rutile) and of $MgSiO_3$ (pyroxene → ilmenite) from high-temperature calorimetry (*47, 48*), and preliminary estimate of $\Delta H^\circ \sim \Delta G^\circ$ for $MgSiO_3$ (ilmenite → perovskite) from high-pressure data (Navrotsky, unpublished calculations).

Perovskite-type $CaGeO_3$ and $CdGeO_3$ are stable only at high pressures. The heats of formation were estimated from recent high-temperature calorimetry of polymorphs of $CaGeO_3$ (*16*) and of $CdGeO_3$ (*17*), combined with the heats of solution of CaO (*18*), GeO_2 (rutile type) (*19*), and CdO in the $2PbO \cdot B_2O_3$ solvent. The heat of solution of CdO in $2PbO \cdot B_2O_3$, not previously reported, was determined in the present work [ΔH°_{sol} (987 K) = 8.70 ± 1.57 kJ/mole]. The heat of formation of $MgSiO_3$ (perovskite) is a crude estimate based on high-pressure data (*46–48*). Note that $CdGeO_3$ and $MgSiO_3$ perovskites are unstable energetically with respect to a mixture of binary oxides at 1 atm.

The apparent nonexistence of $CdZrO_3$ perovskite is consistent with the trends shown in Table IV. All the zirconates studied appear to have heats of formation 30–60 kJ/mole less negative than the corresponding titanates. This trend would place the heat of formation of $CdZrO_3$ between 0 and +30 kJ/mole, indicating no energetic stabilization for this material.

Crystal–Chemical Systematics

The tolerance factor defined by Goldschmidt (*20*) is a useful parameter related to the stability of perovskite structures. It is given by

$$t = (r_A + r_O)/2(r_B + r_O) \qquad (4)$$

where r_A, r_B, and r_O are empirical radii of the respective ions. By geometry, the ideal cubic structure should have $t = 1$. Navrotsky has shown that the heat of formation from oxides of perovskite compounds become less negative in a nearly linear relation with the absolute value of $1 - t$ (*21*). Perovskites ($CdGeO_3$, $CaGeO_3$, and $MgSiO_3$) stable only at high pressure have standard enthalpies of formation from the oxides that are much less negative than the above correlation would suggest (−33 kJ for $CaGeO_3$, +23 kJ for $CdGeO_3$ and an estimated value of +31 ± 20 kJ for $MgSiO_3$). Clearly, at 1 atm these perovskites are rather unstable, and qualitatively this instability probably relates to the rather small size of Mg^{2+} for the central site and of Si^{4+} and Ge^{4+} for the octahedral sublattice.

The concept of tolerance factor is complicated by the fact that ionic radius (and metal–oxygen bond length) depends on coordination number. The numerical value of the tolerance factor therefore depends on whether one considers A^{2+} to be 12-coordinated (as it would be in the ideal cubic structure) or to have a lower coordination number (as low as 8) in a distorted structure. Should one consider perovskite stability in terms of tolerance factors before or after such a distortion occurs?

Because of these questions, we now take a somewhat different approach based on lattice energies. For an ionic crystal, the internal energy can be separated into two terms

$$E = E_M + E_N \qquad (5)$$

where E_M is the electrostatic or Madelung energy and E_N contains all the other terms, of which the repulsive interaction is the largest (positive) contribution, but terms related to Van der Waals energy, vibrational energy, and specific directional (covalent) interactions may contribute. Then, the heat of formation of a perovskite compound can be divided into two parts

$$\Delta H_f \simeq \Delta E = \Delta E_M + \Delta E_N \qquad (6)$$

where ΔE_M is the difference of Madelung energy between product and reactants in reaction (3), while ΔE_N is the difference of repulsion and other energy. If the ΔE_M term is calculated, we can obtain the ΔE_N term using experimental values of ΔH_f according to Eq. (6).

The Madelung energy may be calculated as

$$E_M = 1389M/R_0 \text{ (kJ/mole)} \qquad (7)$$

where M is the Madelung constant and R_0 is the shortest interatomic distance and the numerical factor arises from physical constants and conversion factors. The Madelung constant for the cubic perovskite structure of $A^{2+}B^{4+}O_3$ type is 24.755 (*22*). To calculate the Madelung energy of noncubic perovskites, a simple approximation was used; that is, every compound was treated as ideal cubic perovskite having an average lattice parameter

$$a' = (V_c/z)^{1/3} \quad (8)$$

where V_c is cell volume at room temperature and z is the number of molecules of ABO_3 per unit cell. In this approximation, the shortest interatomic distance, R_0, becomes $a'/2$. We feel that this simple approach is more general for comparative purposes than trying to calculate electrostatic energies of distorted perovskites. The distortions themselves do not result from primarily coulombic interactions and are not known in detail at high T and P. The above computation assumes formal ionic charges.

The Madelung energies of the alkali earth monoxides and CdO were calculated from the Madelung constant for the NaCl-type structure (*22*). The Madelung energies of other compounds, TiO_2 (rutile), GeO_2 (rutile type), SiO_2 (rutile type), ZrO_2 (baddeleyite), and PbO (yellow form), were calculated in the present study by the Ewald method using programs written by A. Yamamoto of NIRIM and K. Leinenweber of Princeton.

TABLE V

THE MADELUNG AND NONCOULOMBIC (REPULSION) ENERGY (kJ/mole)

Compound	E_M[a]	ΔE_M[b]	ΔE_N[c]	Ref.[d]
$CaTiO_3$	−17,986[e]	−322	241	(*23*)
$SrTiO_3$	−17,615	−225	90	(*24*)
$BaTiO_3$	−17,160	−27	−125	(*25*)
$PbTiO_3$	−17,275	58	−89	(*26*)
$CdTiO_3$	−18,071	−308	286	(*27*)
$CaZrO_3$	−17,156	−392	361	(*28*)
$SrZrO_3$	−16,771	−281	205	(*29*)
$BaZrO_3$	−16,406	−173	49	(*30*)
$PbZrO_3$	−16,591	−158	160	(*31*)
$CaGeO_3$	−18,478	−237	204	(*32*)
$CdGeO_3$	−18,567	−227	250	(*33*)
$MgSiO_3$	−20,017	−364	395	(*50*)
MgO	−4,612			(*51*)
CaO	−4,038			(*34*)
SrO	−3,764			(*35*)
BaO	−3,507			(*36*)
CdO	−4,137			(*37*)
PbO	−3,707[f]			(*38*)
TiO_2	−13,626[g]			(*39*)
ZrO_2	−12,726[h]			(*40*)
GeO_2	−14,203[g]			(*39*)
SiO_2	−15,041[g]			(*52*)

[a] Madelung energy calculated using formal ionic charges.

[b] Madelung energy change for reaction $AO + BO_2 = ABO_3$.

[c] Noncoulombic contribution to enthalpy of formation, $\Delta E_N = \Delta H_f - \Delta E_M$.

[d] Reference for lattice parameter and crystal structure.

[e] Madelung energy for perovskite compound was calculated on the assumption of ideal cubic structure.

[f] Madelung energy for yellow form.

[g] Madelung energy for rutile-type structure.

[h] Madelung energy for baddeleyite structure.

Table V shows the Madelung energies of perovskites and values of ΔE_M and ΔE_N calculated by Eqs. (6) and (7). The change in Madelung (electrostatic) energy ΔE_M is negative for all perovskites studied except $PbTiO_3$. It spans a large range (−392 to 58 kJ). The change in nonelectrostatic energy for perovskite formation is positive except for $BaTiO_3$ and $PbTiO_3$. It spans a large range (−125 to 395 kJ) for the compounds studied. The generally positive values of ΔE_N suggest that repulsions increase on forming perovskites from binary oxides. If one considers the perovskite structure ($t <$ 1) to consist of an octahedral sublattice with tetravalent ions and oxygens in contact, and divalent ions filling the large central site, then the lattice constant for the cubic perovskite is related to the ionic radii by the formula (*41*)

$$a_{calc} = 2(r_B + r_O). \quad (9)$$

The calculated lattice constant from this equation is 4.01 Å for titanates, 4.24 Å for zirconates, 3.86 Å for germanates, and 3.60 Å for silicates, using Shannon and Prewitt's revised effective octahedral ionic radii for B^{4+} and O^{2-} (*42*). The observed lattice constant, a_{obs} (for noncubic perovskite, we use the cubic root of cell volume described previously) is, however, usually smaller than a_{calc} (*41*). It seems that in the perovskite structure, the octahedral sublattice is somewhat compressed relative to that predicted by "ideal" M^{4+}–O distances calculated from ionic radii. Of course much of this apparent compression is accounted for by tilting of the octahedra in noncubic perovskites rather than by shorter *B*–O bond lengths. Nevertheless, the calculated apparent compression is an indication of size mismatch. (The values of $\Delta a = a_{calc} - a_{abs}$ would be smaller by ~0.1 Å, but generally similar in their variation with composition, if one used the radius for oxygen in twofold rather than sixfold coordination, that is, if one did not count the longer A^{2+}–O distances as nearest-neighbor distances to oxygen.)

Figure 1 shows both ΔE_M and ΔE_N as functions of Δa. The electrostatic energy change for perovskite formation becomes more negative (more favorable) as Δa increases, while ΔE_N becomes more positive (destabilizing). The systematic trend seen in ΔE_N suggests that changes in repulsive energies are indeed the dominant contribution to ΔE_N. The energy of formation of a

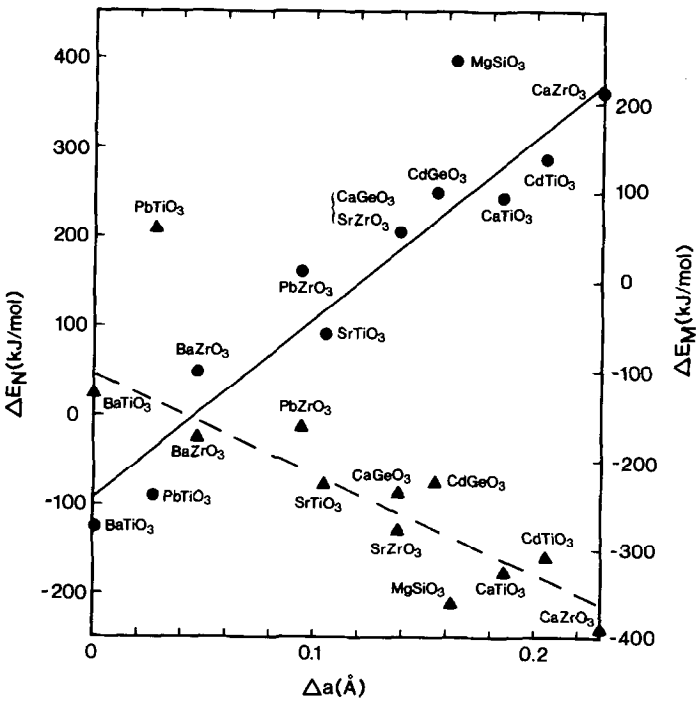

FIG. 1. The triangles, dashed line, and right-hand scale show the relationship between the change in Madelung energy (ΔE_M) upon perovskite formation and the difference between calculated and observed lattice parameters, Δa (see text). The circles, solid line, and left-hand scale show the relationship between the change in nonelectrostatic (largely repulsive) energy and Δa (see text).

perovskite from the binary oxides results from a balance of ΔE_M and ΔE_N terms, which depend in opposite fashions on Δa (see Fig. 1).

For comparison, Fig. 2 shows ΔE_M and ΔE_N plotted against the tolerance factor, t, defined by Eq. (4). Somewhat arbitrarily, but to be consistent with most observed coordination numbers in perovskites, we have chosen coordination numbers of 6 for oxygen and the tetravalent ions, 8 for the smaller divalent ions (Mg, Cd, Ca), and 12 for the larger divalent ions (Sr, Pb, Ba). Using this convention, values of t are slightly greater than unity for $SrTiO_3$, $BaTiO_3$, and $PbTiO_3$. Both ΔE_M and ΔE_N show correlation with t, the electrostatic energy change becoming less favorable and the repulsive energy change more favorable

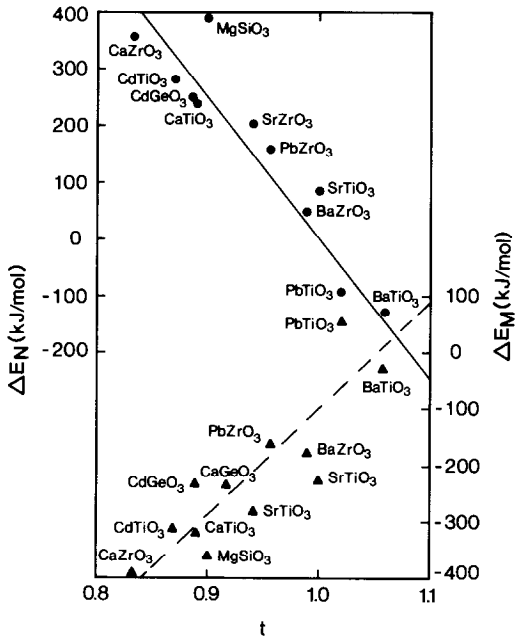

FIG. 2. The triangles, dashed line, and right-hand scale show the relationship between the change in Madelung energy (ΔE_M) upon perovskite formation and the tolerance factor, t (see text). The circles, solid line, and left-hand scale show the relationship between the change in nonelectrostatic (largely repulsive) energy and t (see text).

with increasing t. Qualitatively, the same balance of electrostatic and repulsive energies is seen whether one uses Δa or t as a measure of bond length mismatch in the perovskite structure.

We note that the high-pressure germanate and silicate perovskites fall on the same general trends as the titanates and zirconates, though for $MgSiO_3$ the change in nonelectrostatic energy may be some 50 kJ more destabilizing than the trend would predict; however, the heat of formation of that compound is an estimated value which has large uncertainties.

The perovskite structure is of course not restricted to oxides of the $A^{2+}B^{4+}O_3$ change type. Oxide perovskites of the type $A^{3+}B^{3+}O_3$ and fluoride perovskites of the type $A^{+}B^{2+}F_3$ form extensive families, and many other complex perovskites are known. The presently available thermochemical data are insufficient to test whether systematics similar to those observed here apply to the other charge types. The perovskite-forming reaction is different for other charge types because some of the binary oxides and fluorides have different structures. Additional systematic thermochemical studies are needed to further characterize the patterns of stability of this ubiquitous structure.

Ilmenite–Perovskite Transition in $CdTiO_3$

The ilmenite–perovskite transition in $CdTiO_3$ was investigated in solid-state high-pressure and hydrothermal experiments by Liebertz and Rooymans (*5*). By applying the Clausius–Clapeyron equation, they estimated $\Delta S = 14.2$ J/mole · K for the reaction

$$CdTiO_3 \text{ (ilmenite)} \rightarrow CdTiO_3 \text{ (perovskite)} \quad (10)$$

Strong kinetic inhibitions, however, made it difficult to get an unambiguous phase boundary from their experimental runs alone.

High-temperature solution calorimetry using $3Na_2O \cdot 4MoO_4$ solvent has been applied to the $CdTiO_3$ polymorphs to obtain the enthalpy of reaction (10) (*15*). The result ($\Delta H^\circ_{965} = 15.0 \pm 0.8$ kJ/mole) is in good agreement with the 15.6 kJ/mole estimated from the entropy change and transition temperature at 1 atm (1103 K), supporting the experimental phase boundary. An interesting point is that ΔS and ΔV have opposite signs, and the denser polymorph appears as the high-temperature form in the phase diagram. This phenomenon has been explained by a large vibrational entropy of the perovskite form arising from less rigid binding of the relatively small Cd^{2+} ion (*15*).

On the other hand, using the present ΔH°_{sol} for the two polymorphs, we calculate $\Delta H^\circ_{1068} = 8.2 \pm 2.3$ kJ/mole for reaction (10). This value is significantly smaller than the previous ones, and is in conflict with the phase boundary of Liebertz and Rooymans. One possible reason for the discrepancy in calorimetric data may be experimental problems in the earlier solution experiments, since it is difficult to dissolve TiO_2-bearing samples completely in $3Na_2O \cdot 4MoO_3$ (*9*). To check the new value of ΔH, an independent calorimetric method (transposed-temperature-drop calorimetry) was applied to the $CdTiO_3$ polymorphs. Using the results shown in Table VI, ΔH°_{298} for reaction (10) was calculated to be 10.2 ± 4.8 kJ/mole from the experiment at 1333 K and 9.09 ± 3.33 kJ/mole from the experiment at 1353 K. Since there is practically no difference in heat content, $\Delta H^\circ_{1068} - H^\circ_{298}$, between ilmenite and perovskite forms, we can conclude that $\Delta H^\circ_{298} \simeq \Delta H^\circ_{1068}$ for reaction (10). The results of transposed-temperature-drop calorimetry support the value of ΔH in the present solution experiments rather than in the earlier ones.

From the present ΔH°_{1068} from solution calorimetry and the transition temperature at 1 atm, the entropy change was determined to be 7.5 ± 2.1 J/mole · K. The entropy change still has the sign opposite that of the volume change. The source of the discrepancy with the phase studies is unclear. Additional work is needed.

TABLE VI

CALORIMETRIC DATA FOR $CdTiO_3$ POLYMORPHS OBTAINED BY TRANSPOSED-TEMPERATURE-DROP CALORIMETRY

Reaction	ΔH° (kJ/mol)
il(298 K)[a] → il(1068 K)	90.4 ± 0.5(4)[b,c]
pv(298 K)[d] → pv(1068 K)	90.3 ± 0.2(3)
il(298 K) → pv(1333 K)	133.0 ± 4.7(8)
pv(298 K) → pv(1333 K)	122.8 ± 1.1(4)
il(298 K) → pv(1353 K)	138.2 ± 2.4(14)
pv(298 K) → pv(1353 K)	129.1 ± 2.3(14)

[a] $CdTiO_3$ (ilmenite).
[b] Error is standard deviation.
[c] Number in parentheses is number of experiments performed.
[d] $CdTiO_3$ (perovskite).

Transition between $BaTiO_3$ (Perovskite) and $BaTiO_3$ (Hexagonal)

Barium titanate, $BaTiO_3$ has five crystalline forms, of which four are of the perovskite type. The high-temperature hexagonal form is stable from 1733 K to the melting point (*7*). In the hexagonal form, Ba and Ti ions occupy 12-fold and 6-fold sites, respectively, as they do in perovskite. The most important difference in the hexagonal structure is the presence of Ti_2O_9 groups, that is, face-sharing occurs between two TiO_6 octahedra (*43*).

From solution calorimetry of the two polymorphs of $BaTiO_3$, $\Delta H^\circ_{1068} = 5.6 \pm 3.4$ kJ/mole for the reaction

$$BaTiO_3 \text{ (perovskite)} \rightarrow BaTiO_3 \text{ (hexagonal)}. \quad (11)$$

The entropy change for this transition could be calculated using the transition temperature at 1 atm (1733 K),

$$\Delta S^\circ \simeq H^\circ_{1068}/1733 = 3.2 \pm 2.0 \text{ J/mole} \cdot \text{K} \quad (12)$$

The positive value of the enthalpy change may be related to the existence of the Ti_2O_9 group, which may give the hexagonal form a higher repulsive energy. The positive entropy change is required since the hexagonal form is the one stable at high temperature. For the cubic → hexagonal transition, both ΔS° and ΔV° are positive, with $\Delta V^\circ_{298} = 1.00$ cm^3/mole (*25, 44*).

Acknowledgments

The authors thank A. Yamamoto and K. Leinenweber for calculating Madelung energies and H. Yamamura and B. Wechsler for offering $BaTiO_3$ samples. This work was supported by the National Science Foundation (Grants DMR 8106027 and 8521562 from the Solid State Chemistry Program). We thank Mrs. M. Kobayashi and Mr. Y. Yajima of NIRIM for the chemical analyses.

References

1. J. B. Goodenough and J. M. Longo, *in* "Landolt–Bornstein, Numerical Data and Functional Relationships in Science and Technology, New Series" (K. H. Hellwege and A. M. Hellwege, Eds.), Vol. 4a, p. 126, Springer-Verlag, Berlin/Heidelberg/New York (1970).
2. R. Jeanloz and A. B. Thompson, *Rev. Geophys. Earth Phys.* **21,** 51 (1983).
3. E. Ito and Y. Matsui, *Phys. Chem. Min.* **4,** 265 (1979).
4. A. Navrotsky, *Phys. Chem. Min.* **2,** 89 (1977).
5. J. Liebertz and C. J. M. Rooymans, *Z. Phys. Chem. N.F.* **44,** 242 (1956).
6. W. S. Clabaugh, E. M. Swiggard, and R. Gilchrist, *J. Res. Natl. Bur. Stand.* **56,** 289 (1965).
7. D. E. Rase and R. Roy, *J. Chem. Phys.* **38,** 102 (1955).
8. "Gmelin's Handbuch der anorganischen Chemie," 8th ed., System No. 30, p. 297, Verlag Chemie, Weinheim (1960).
9. B. A. Wechsler and A. Navrotsky, *J. Solid State Chem.* **55,** 165 (1984).
10. C. Chatillon-Colinet, O. J. Kleppa, R. C. Newton, and D. Perkins III, *Geochim. Cosmochim. Acta* **47,** 439 (1983).
11. A. Navrotsky, R. Hon, D. F. Weill, and D. J. Henry, *Geochim. Cosmochim. Acta* **44,** 1409 (1980).
12. A. Navrotsky, J. C. Jamieson, and O. J. Kleppa, *Science* **158,** 388 (1977).
13. E. Takayama-Muromachi, A. Navrotsky, and S. Yamaoka, *J. Solid State Chem.* **68,** 241 (1986).
14. O. V. Kedrovskii, I. V. Kovtunenko, E. V. Kiseleva, and A. A. Bundel, *Russ. J. Phys. Chem.* **41,** 205 (1967). [English translation]
15. J. M. Neil, A. Navrotsky, and O. J. Kleppa, *Inorg. Chem.* **10,** 2076 (1971).
16. N. L. Ross, M. Akaogi, A. Navrotsky, J. Susaki, and P. McMillan, *J. Geophys. Res.* **91,** 4685 (1986).
17. M. Akaogi and A. Navrotsky, *Phys. Chem. Min.* **14,** 435 (1987).
18. A. Navrotsky and W. E. Coons, *Geochim. Cosmochim. Acta* **40,** 1281 (1976).
19. A. Navrotsky, *J. Inorg. Nucl. Chem.* **33,** 1119 (1971).
20. V. M. Goldschmidt, *Skr. Nor. Vidensk-Akad. Oslo* **1,** 1 (1926).
21. A. Navrotsky, *in* "Structure and Bonding in Crystals" (M. O'Keeffe and A. Navrotsky, Eds.), Vol. II, p. 71, Academic Press, New York (1981).
22. Q. C. Johnson and D. H. Templeton, *J. Chem. Phys.* **34,** 2004 (1961).
23. Joint Committee on Powder Diffraction Standards, No. 22–153.
24. Joint Committee on Powder Diffraction Standards, No. 35–734.
25. Joint Committee on Powder Diffraction Standards, No. 5–626.
26. Joint Committee on Powder Diffraction Standards, No. 6–452.
27. H. F. Kay and J. L. Miles, *Acta Crystallogr.* **10,** 213 (1957).
28. Joint Committee on Powder Diffraction Standards, No. 35–790.
29. Joint Committee on Powder Diffraction Standards, No. 10–268.
30. Joint Committee on Powder Diffraction Standards, No. 6–399.
31. Joint Committee on Powder Diffraction Standards, No. 35–739.
32. S. Sasaki, C. T. Prewitt, and R. C. Liebermann, *Amer. Mineral.* **68,** 1189 (1983).
33. J. Suzaki and S. Akimoto, Abstract of the 24th High Pressure Conference of Japan, p. 130 (1983). [in Japanese]
34. Joint Committee on Powder Diffraction Standards, No. 4–777.
35. Joint Committee on Powder Diffraction Standards, No. 6–520.

36. Joint Committee on Powder Diffraction Standards, No. 22–1056.
37. Joint Committee on Powder Diffraction Standards, No. 5–640.
38. R. W. G. WYCKOFF, "Crystal Structures," 2nd ed., Vol. 1, p. 137, Wiley, New York/London/Sydney (1967).
39. R. W. G. WYCKOFF, "Crystal Structures," 2nd ed., Vol. 1, p. 251, Wiley, New York/London/Sydney (1967).
40. R. W. G. WYCKOFF, "Crystal Structures," 2nd ed., Vol. 1, p. 244, Wiley, New York/London/Sydney (1967).
41. O. FUKUNAGA AND T. FUJITA, *J. Solid State Chem.* **8,** 331 (1973).
42. R. D. SHANNON AND C. T. PREWITT, *Acta Crystallogr. Sect. A* **32,** 751 (1976).
43. R. D. BURBANK AND H. T. EVANS, JR., *Acta Crystallogr.* **1,** 330 (1948).
44. Joint Committee on Powder Diffraction Standards, No. 34–129.
45. I. BARIN AND O. KNACKE, "Thermochemical Properties of Inorganic Substances," Springer-Verlag, Berlin/Heidelberg/New York (1973); I. BARIN, O. KNACKE, AND O. KUBASCHEWSKI, "Thermochemical Properties of Inorganic Substances, Supplement," Springer-Verlag, Berlin/Heidelberg/New York (1977).
46. T. V. CHARLU, R. C. NEWTON, AND O. J. KLEPPA, *Geochim. Cosmochim. Acta* **39,** 1487 (1975).
47. M. AKAOGI AND A. NAVROTSKY, *Phys. Earth Planet. Int.* **56,** 124 (1984).
48. E. ITO AND A. NAVROTSKY, *Amer. Mineral.* **70,** 1020 (1985).
49. T. MITSUHASHI AND O. J. KLEPPA, *J. Amer. Ceram. Soc.* **62,** 356 (1979).
50. E. ITO AND Y. MATSUI, *Earth Planet. Sci. Lett.* **38,** 443 (1978).
51. Joint Committee on Powder Diffraction Standards, No. 4-829.
52. W. SINCLAIR AND A. E. RINGWOOD, *Nature (London)* **272,** 714 (1978).
53. J. G. BEDNORZ AND K. A. MULLER, *Z. Phys. B* **64,** 189 (1986).